coatings

MDPI

Article

Effect of Mechanical Properties of Substrates on Flexibility of Ag Nanowire Electrodes under a Large Number of Bending Cycles

Tae Gwang Yun [1] and Byungil Hwang [2,*]

[1] Department of Materials Science and Engineering, Myongji University, Yongin 17058, Korea; ytk0402@mju.ac.kr
[2] School of Integrative Engineering, Chung-Ang University, Seoul 06974, Korea
* Correspondence: bihwang@cau.ac.kr

Abstract: Ag nanowire electrodes have attracted considerable attention because of their potential applications in next-generation flexible electronics. However, there is a paucity of studies on the mechanical properties of Ag nanowire electrodes subjected to a large number of bending cycles. In this study, the effects of the substrate on the mechanical behavior of Ag nanowire electrodes were studied for a high bending frequency. The mechanical reliability of the Ag nanowire electrodes fabricated on a polyethylene terephthalate (PET) substrate was better than that for a polyimide (PI) substrate; the increase in the resistance of the PET-based Ag nanowire electrode was 1.07%, while that of the PI-based one was 1.23%. Nanoindentation tests showed that the elastic modulus of PI was larger than that of PET. This resulted in a lower bending strain on PET-based Ag nanowire electrodes compared to those on PI-based ones, because of the smaller distance from the neutral plane of the PET-based system. Our study showed that the mechanical properties of the substrate influenced the strain imposed on the thin layer on the substrates, which, in turn, determines the mechanical reliability of the thin-layer/substrate multilayer system.

Keywords: bending; neutral plane; Ag nanowire; reliability; substrate

check for updates

Citation: Yun, T.G.; Hwang, B. Effect of Mechanical Properties of Substrates on Flexibility of Ag Nanowire Electrodes under a Large Number of Bending Cycles. *Coatings* **2021**, *11*, 1074. https://doi.org/10.3390/coatings11091074

Academic Editor: Robert Zierold

Received: 19 August 2021
Accepted: 3 September 2021
Published: 6 September 2021

Publisher's Note: MDPI stays neutral with regard to jurisdictional claims in published maps and institutional affiliations.

Copyright: © 2021 by the authors. Licensee MDPI, Basel, Switzerland. This article is an open access article distributed under the terms and conditions of the Creative Commons Attribution (CC BY) license (https://creativecommons.org/licenses/by/4.0/).

1. Introduction

Technological advances in flexible electronics require reliable, flexible transparent electrodes that are stable under severe deformation, when subjected to a large number of bending cycles [1–3]. Indium tin oxide (ITO) has a high optical transmittance and electrical conductivity, as well as excellent thermal and chemical stabilities; thus, it is the most widely used material for transparent electrodes [4–6]. However, ITO requires a high processing temperature, which is unsuitable for flexible substrates that are mostly constructed using polymeric materials [4–6]. In addition, the mechanical brittleness of ITO limits its use in flexible electronics [7,8]. To overcome these limitations, several ITO alternatives have been reported, including graphene [9,10], carbon nanotubes [11,12], metal meshes [13,14], and metal nanowires [15,16]. Among them, Ag nanowires are considered to be the most promising alternative because of their good optical and electrical performance, scalable synthesis, and ease of coating to form electrodes [17,18]. Furthermore, the network structure of Ag nanowires can make them highly flexible under bending deformation [19,20]. With the increasing interest in Ag nanowire electrodes, there have been many studies on the synthesis of Ag nanowires or applications of Ag nanowires in flexible electronics [21,22]. However, for the commercial use of Ag nanowires, their mechanical reliability under different deformations should be understood, especially under a large number of bending cycles.

There have been several reports on the evaluation of the mechanical properties of Ag nanowire electrodes subjected to bending [23–25]. For example, Jin et al. reported

Ag nanowire transparent electrodes for application in flexible transparent heaters; bending tests were performed to confirm the flexibility of the electrodes under 100 cycles of bending [23]. There was no significant change in resistance during bending. Chen et al. demonstrated Ag nanowire electrodes on a polyethylene terephthalate (PET) substrate, for application as a biosensor [24]. To confirm the mechanical stability, 100,000 bending cycles, under a 5 mm radius, were imposed on the electrodes, which resulted in a negligible change in resistance during bending. Hao et al. also fabricated Ag nanowire/PET transparent electrodes and performed bending tests up to 2000 cycles at an angle of 180° [25]. In this work, the resistance of the Ag nanowire electrodes was increased by 60% after 2000 bending cycles. Although there have been several studies on Ag nanowire transparent electrodes, as indicated in the examples, most of them were performed by imposing only a limited number of bending cycles, which makes it difficult to delineate the mechanical behavior of the Ag nanowire electrodes under bending. In addition, the changes in resistance, owing to bending, were neglected; however, this contradicts real-life situations, especially in industrial applications where the reliability of the product is one of the most important factors. Furthermore, the substrate materials influence the mechanical behavior of the electrodes, owing to the different bending strains that arise from the differences in the mechanical properties of the substrates. Therefore, studies on the effect of the substrate on the mechanical behavior of Ag nanowire electrodes need to be expedited.

In this work, a systematic study of the deformation behavior of Ag nanowire electrodes was performed using a cyclic bending tester. While imposing bending deformation up to 400,000 cycles, the change in resistance was measured in situ and correlated with the deformation of the Ag nanowires during bending. Polyimide (PI) and PET, which are the two most widely used substrates, were used to study the effect of the substrates on the deformation behavior of Ag nanowire electrodes.

2. Experimental Section

2.1. Sample Preparation

An Ag nanowire suspension in isopropyl alcohol was purchased from Nanopyxis and used as received. The average diameter and length of the Ag nanowires were ~35 nm and 15 μm, respectively. PI films (Kepton E, Dupont) with 125 μm thickness and PET films (Kolon) were used as received. The Ag nanowires were deposited on the substrates using an air spray system (NanoNC). The fabricated Ag nanowire electrode had an initial sheet resistance of 41.3 ± 2.9 Ω/sq. Post-annealing was performed on the samples placed in a box furnace at 100 °C for 60 min. Further, 2~3 nanowires were stacked to form the networks; thus, the thickness of the Ag nanowire networks could be considered as ~100 nm. A 100-nm-thick Ag thin film was deposited using DC magnetron sputtering at 100 W for 20 min at room temperature. Scanning electron microscopy (SEM, Phillips, XL30 ESEM–FEG, Hillsboro, OR, USA) was used to characterize the microstructures of the specimens.

2.2. Characterization

For cyclic bending tests, a cyclic bending tester (CK Tradings) with a resolution of ~0.003 Ω, capable of in situ resistance monitoring, was employed. Ag nanowire electrodes on PI or PET substrates were fixed between the upper and bottom plates using metal bolts to conduct the bending tests. The fluctuations in the electric signal during cyclic bending can be collected in situ at the edge connected to the copper electrodes by metal bolts. The strain applied to the sample was calculated using the equation $\varepsilon = y/R$, where ε, y, and R are the bending strain, distance from the neutral plane, and bending radius, respectively. The industrial criterion for the bending radius is generally 3.0 mm; thus, the bending radius for this study was fixed at 2.0 mm for more severe deformation. Three hundred bending cycles were imposed on the samples per minute. A more detailed explanation of the cyclic bending tester can be found in [26,27].

Nanoindentation (MTS, Nano Indenter XP) with a Berkovich tip was used to characterize the mechanical properties of the PI and PET substrates. The tests were performed using a continuous stiffness measurement method in a load-controlled mode with a maximum load of 100 mN. Sixteen positions were indented per sample to confirm the reliability of the results. The hardness and the elastic modulus were calculated using the Oliver and Pharr model, which is explained in detail in Ref. [28].

3. Results and Discussion

The normalized resistance changes $((R-R_0)/R_0)$ of the PI and PET substrate-based Ag nanowire electrodes, when subjected to 400,000 cycles of bending, are shown in Figure 1a. Overall, the Ag nanowire electrodes on both the PI and PET substrates exhibited excellent mechanical reliability under bending, showing an increase of only ~1.23% and ~1.07% in resistance for the PI and PET substrate samples, respectively. Considering that Ag thin films with a similar thickness of ~100 nm on PI and PET substrates exhibited increases in resistance of approximately 184% and 122%, respectively, under the same bending conditions as those for the Ag nanowire samples, the observed values were extremely low, indicating the excellent mechanical reliability of the Ag nanowire electrodes. We have repeated the tests for each sample five times, which showed similar results with a low deviation of ~0.02%. The excellent reliability of Ag nanowire electrodes may be attributed to the following two factors: (1) the geometrical advantages of the network structure that can accommodate the bending strain by stretching the network structure, and (2) the benefit of nanoscale nanowires that prevent void or protrusion formation at the film/substrate interfaces, due to the dislocation starvation effect. Crack formation in metallic thin films is the main reason for the increase in resistance under repeated bending [26,29]. The repeated plasticity causes the accumulation of dislocations at the interfaces between the metallic thin film and substrate, which results in void formation at the interfaces. The cluster of voids, formed in response to the repeated bending strain, created protrusions in regions of stress concentration, which initiated microcracks in the thin films. As the crack density is increased by the continuous bending strains, the cracks collapse and propagate, resulting in long-range cracks through the metallic thin films. The cracks hindered the current flow, causing a rapid increase in the resistance of the film under cyclic bending, as shown in Figure 1b.

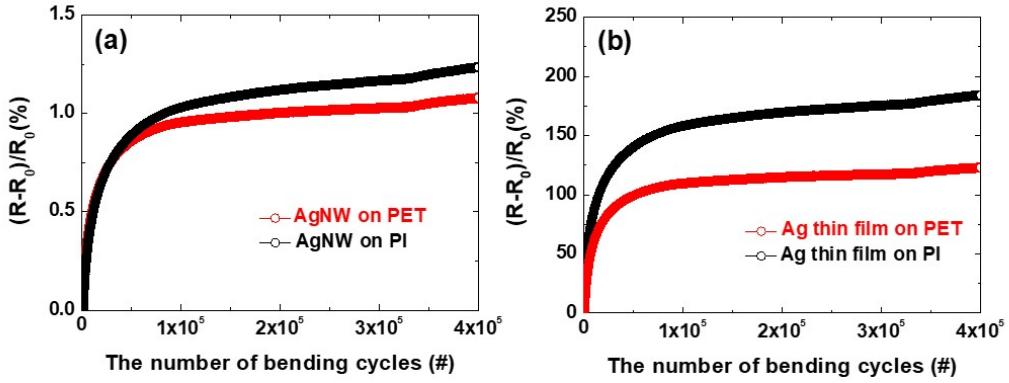


Figure 1. Normalized resistance change under cyclic bending of (**a**) Ag nanowire electrodes and (**b**) Ag thin films on PI and PET substrates.

In contrast, the increase in resistance in the Ag nanowire networks resulted from the failure of the nanowires [30]. Figure 2 shows the SEM images of the Ag nanowire electrodes on PI and PET substrates before and after the cyclic bending tests. Without bending, the Ag nanowires were stacked as shown in Figure 2a,b. There were no clear differences in the microstructures of the different substrates. After 400,000 cycles of bending, disconnected nanowire networks were observed intermittently throughout the samples, which is the main reason for the increase in the resistance of the Ag nanowire electrodes. However,

continuous long-range failures were hardly observed. Ag nanowire networks on polymer substrates were not strongly bound to the substrates, unlike metallic thin films [8,31]. Thus, they have relatively greater freedom to transform their geometry than blanket metal thin films that are formed on polymer substrates. Upon bending, Ag nanowire networks can stretch out their geometry to effectively accommodate the bending strain, thereby reducing the imposed strain on the individual nanowires [19]. In addition, the accumulation of dislocations in the Ag nanowire networks on polymer substrates is difficult, owing to the well-known dislocation starvation effect [32,33]. In the nanoscale diameter of Ag nanowires, the initiated or pre-existing dislocation glides out of the nanowire before multiplying, because the distance for dislocation breeding is comparable to or larger than the nanowire diameter [32]. Thus, the probability of dislocation build-up is much less than that in the metallic thin film, which reduces the possibility of network failure. Furthermore, the space between the individual nanowires can retard the propagation of failure through the networks [34], which will reduce the formation of long-range failures through the entire width or length of the networks.

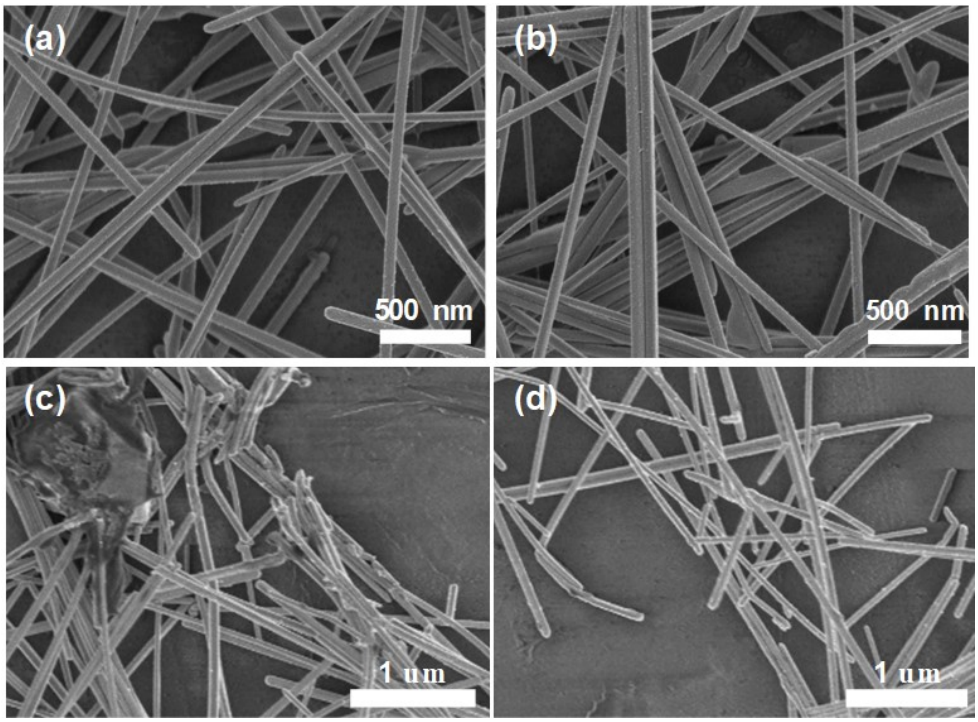


Figure 2. Plan view SEM images taken for Ag nanowire electrodes on (**a**) PI and (**b**) PET substrates before bending and on (**c**) PI and (**d**) PET substrates after 400,000 cycles of bending.

Even though Ag nanowire electrodes show excellent mechanical reliability under cyclic bending, the difference in the resistance increase between the PI and PET samples should be discussed in detail. As shown in Figure 1a, the increase in the resistance of Ag nanowire electrodes on PI and PET substrates after 40,000 bending cycles were ~1.23% and ~1.07%, respectively. The values for the PI substrate samples were ~0.16% larger than those associated with the PET substrates. To discuss the differences resulting from the substrates, the imposed strain on the Ag nanowire electrodes, caused by the different substrates, should be discussed. Under the bending of the multilayered structure, the imposed strain on the thin layer on the compliant substrates under bending can be calculated using the equation $\varepsilon = y/R$, where ε, y, and R are the bending strain, distance from the neutral plane, and bending radius, respectively. In our experiments, the bending radius was fixed as a single value for both Ag nanowires on PI and PET substrates; thus, the location of

the neutral plane is the only difference, which needs to be calculated for both samples (Figure 3).

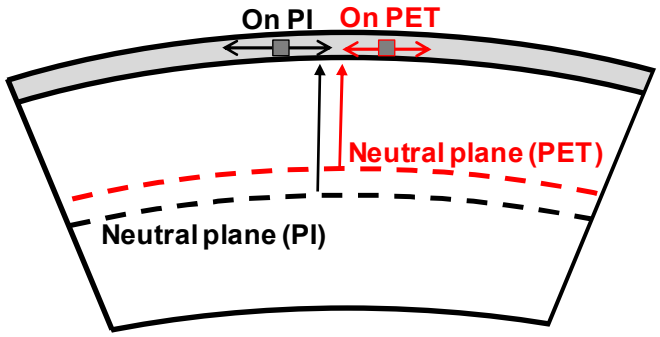


Figure 3. Schematic of the imposed strain on the sample on the different substrates.

According to the equation $S = \frac{\sum_{i=0}^{n} B_i\left(y_{i+1}^2 - y_i^2\right)}{2\sum_{i=0}^{n} B_i\left(y_{i+1} - y_1\right)}$, where S is the location of the neutral plane, B is the biaxial modulus that is calculated by $E/(1-\nu)$, where E and ν are the elastic modulus and Poisson's ratio, respectively, and $y_{(i+1)} - y_1 = \Delta y$ is the thickness of each layer. The neutral plane position for the given multilayer systems can be calculated. To calculate the location of the neutral plane accurately, the biaxial modulus, which can be calculated with the value of the elastic modulus, must be measured. Nanoindentation tests with a Berkovich tip were performed on the PI and PET substrates, to measure the elastic modulus. Figure 4 shows the elastic modulus of the PI and PET substrates as a function of the tip displacement. The elastic modulus values of the PI and PET substrates were 5.27 ± 0.03 GPa and 3.31 ± 0.05 GPa, respectively. The hardness values of the PI and PET substrates were 0.15 ± 0.01 GPa and 0.23 ± 0.02 GPa, respectively (Figure 5). Using the elastic modulus values, the locations of the neutral planes are calculated, which are 63.7 and 63.1 μm for the PI and PET substrates, respectively. Therefore, the imposed strains on the Ag nanowire electrodes, based on the PI and PET substrates, were calculated to be 3.1% and 3.0%, respectively. The gap between the imposed strain on the PI and PET substrates was ~0.1%. The value itself is not significant; however, considering the cyclic bending condition of more than 400,000 cycles, this small value can affect the mechanical reliability, as observed in the cyclic bending test results in Figure 1a. In addition, the change in the imposed strain can be more significant as the thickness of the substrate increases, or as the structure of the multilayer system changes. For example, the gap between the imposed strain on the Ag nanowire electrodes, based on PI and PET substrates with a thickness of 200 μm, is calculated as ~0.3%, which is three times larger than that for the 125-mm-thick substrates. Therefore, our results indicate that the substrates can modulate the mechanical stability of the flexible devices; thus, the elastic modulus of the substrates should be carefully considered when designing multilayered flexible systems to satisfy the mechanical stability requirements of the devices. It was discussed in our previous study that the mechanical reliability of the Ag nanowire networks in the single type of substrates was better for the thin networks than those of thick samples, due to the reduced strain for the thinner samples [35]. Varying the adhesion of Ag nanowires and polymeric substrates will also cause the differences in the mechanical stability of Ag nanowire networks. However, they are out of the scope of this manuscript. Thus, it will be attractive topic for our future study.

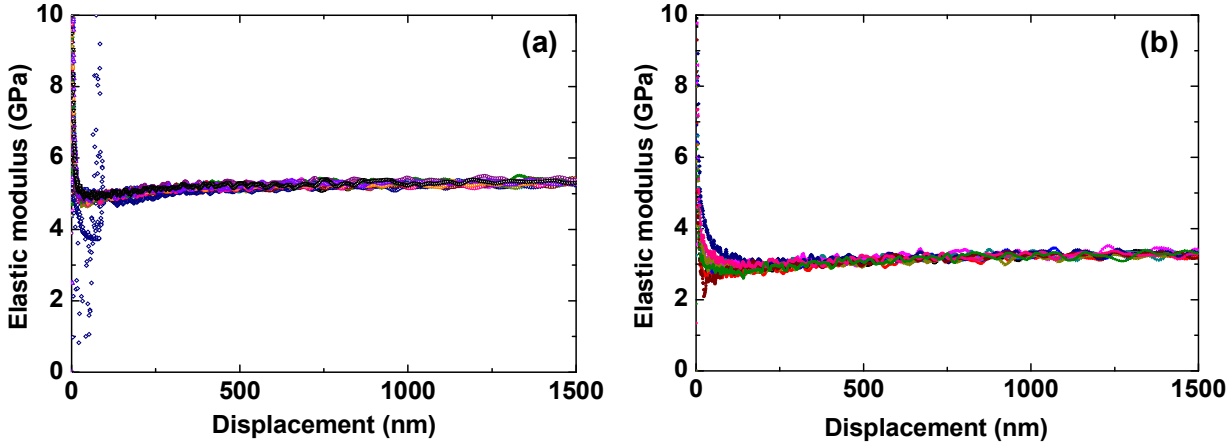


Figure 4. Elastic modulus of (**a**) PI and (**b**) PET substrates. Tests were conducted for 16 positions on samples.

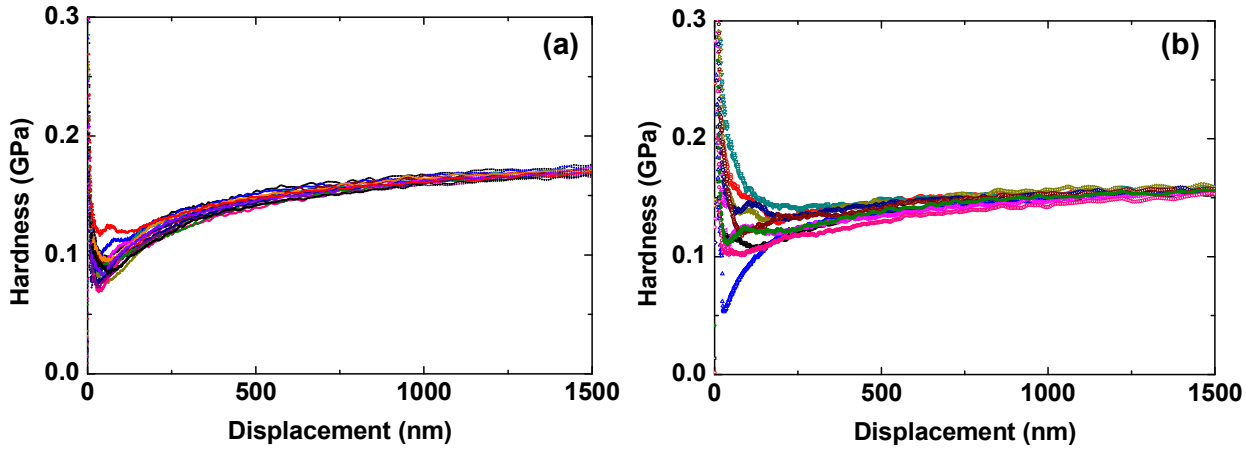


Figure 5. Hardness of (**a**) PI and (**b**) PET substrates. Tests were conducted for 16 positions on samples.

4. Conclusions

In this study, the mechanical stabilities of the Ag nanowire electrodes on PI and PET substrates, which are the most widely used systems in industry, were investigated by imposing repeated bending strains of up to 400,000 cycles. The Ag nanowire electrodes on PI and PET substrates showed excellent mechanical stability of bending, with increases of ~1.23% and 1.07% in the resistance after 400,000 cycles, respectively. The small gaps in the trend of resistance increase for Ag nanowire electrodes on PI and PET substrates were attributed to the different imposed bending strains on the thin Ag nanowire layer, resulting from the different substrates with different elastic moduli. Nanoindentation tests showed that PI substrates had a larger elastic modulus (5.27 $\pm$ 0.03 GPa) than those of PET substrates (3.31 $\pm$ 0.05 GPa). The different elastic moduli resulted in differences of 63.7 and 63.1 μm in the neutral plane position for the PI and PET substrates, respectively. Consequently, the imposed bending strain on the Ag nanowire electrodes on the PI substrates was 0.1% larger than that on the PET substrates. Although the value of the strain gap is not significantly large, such a gap may cause differences in the mechanical stability when the bending stresses exceed 400,000 cycles. Our results reveal that the elastic modulus of the substrate is critical to the reliability of flexible devices with multilayer structures.

Author Contributions: Data curation, T.G.Y. and B.H.; Formal analysis, T.G.Y. and B.H.; Funding acquisition, B.H.; Investigation, T.G.Y. and B.H.; Project administration, T.G.Y. and B.H.; Resources, T.G.Y. and B.H.; Supervision, T.G.Y. and B.H.; Writing—original draft, T.G.Y. and B.H. All authors have read and agreed to the published version of the manuscript.

Funding: This research was supported by the Chung-Ang University Research Grants in 2020 and by the National Research Foundation of Korea (NRF) (No. 2021R1F1A1054886).

Conflicts of Interest: The authors declare no conflict of interest.

References

1. Hu, X.; Meng, X.; Zhang, L.; Zhang, Y.; Cai, Z.; Huang, Z.; Su, M.; Wang, Y.; Li, M.; Li, F. A Mechanically Robust Conducting Polymer Network Electrode for Efficient Flexible Perovskite. *Sol. Cells Joule* **2019**, *3*, 2205–2218. [CrossRef]
2. Jun, S.; Kim, Y.; Ju, B.-K.; Kim, J.-W. Extremely flexible, transparent, and strain-sensitive electroluminescent device based on ZnS:Cu-polyvinyl butyral composite and silver nanowires. *Appl. Surf. Sci.* **2018**, *429*, 144–150. [CrossRef]
3. Park, J.; Hyun, B.G.; An, B.W.; Im, H.-G.; Park, Y.-G.; Jang, J.; Park, J.-U.; Bae, B.-S. Flexible transparent conductive films with high performance and reliability using hybrid structures of continuous metal nanofiber networks for flexible optoelectronics. *ACS Appl. Mater. Interfaces* **2017**, *924*, 20299–20305. [CrossRef] [PubMed]
4. Choi, K.H.; Kim, J.Y.; Lee, Y.S.; Kim, H.J. ITO/Ag/ITO multilayer films for the application of a very low resistance transparent electrode. *Thin Solid Film.* **1999**, *341*, 152–155. [CrossRef]
5. Gross, G.W.; Wen, W.Y.; Lin, J.W. Transparent indium-tin oxide electrode patterns for extracellular, multisite recording in neuronal cultures. *J. Neurosci. Methods* **1985**, *15*, 243–252. [CrossRef]
6. Minami, T. Present status of transparent conducting oxide thin-film development for Indium-Tin-Oxide (ITO) substitutes. *Thin Solid Film.* **2008**, *516*, 5822–5828. [CrossRef]
7. Aleksandrova, M.; Kurtev, N.; Videkov, V.; Tzanova, S.; Schintke, S. Material alternative to ITO for transparent conductive electrode in flexible display and photovoltaic devices. *Microelectron. Eng.* **2015**, *145*, 112–116. [CrossRef]
8. Hwang, B.; An, Y.; Lee, H.; Lee, E.; Becker, S.; Kim, Y.-H.; Kim, H. Highly flexible and transparent Ag nanowire electrode encapsulated with ultra-thin Al2O3: Thermal, ambient, and mechanical stabilities. *Sci. Rep.* **2017**, *7*, 41336. [CrossRef]
9. Wu, J.; Becerril, H.A.; Bao, Z.; Liu, Z.; Chen, Y.; Peumans, P. Organic solar cells with solution-processed graphene transparent electrodes. *Appl. Phys. Lett.* **2008**, *92*, 263302. [CrossRef]
10. Wu, J.; Agrawal, M.; Becerril, H.A.; Bao, Z.; Liu, Z.; Chen, Y.; Peumans, P. Organic light-emitting diodes on solution-processed graphene transparent electrodes. *ACS Nano* **2010**, *4*, 43–48. [CrossRef]
11. Jeon, I.; Yoon, J.; Kim, U.; Lee, C.; Xiang, R.; Shawky, A.; Xi, J.; Byeon, J.; Lee, H.M.; Choi, M.; et al. High-performance solution-processed double-walled carbon nanotube transparent electrode for perovskite. *Sol. Cells* **2019**, *9*, 1901204. [CrossRef]
12. An, C.-H.; Kim, S.; Lee, H.-J.; Hwang, B. Facile patterning using dry film photo-resists for flexible electronics: Ag nanowire networks and carbon nanotube networks. *J. Mater. Chem. C* **2017**, *5*, 4804–4809. [CrossRef]
13. Khan, A.; Lee, S.; Jang, T.; Xiong, Z.; Zhang, C.; Tang, J.; Guo, L.J.; Li, W.-D. High-performance flexible transparent electrode with an embedded metal mesh fabricated by cost-effective solution process. *Small* **2016**, *12*, 3021–3030. [CrossRef]
14. Chen, X.; Guo, W.; Xie, L.; Wei, C.; Zhuang, J.; Su, W.; Cui, Z. Embedded Ag/Ni metal-mesh with low surface roughness as transparent conductive electrode for optoelectronic applications. *ACS Appl. Mater. Interfaces* **2017**, *9*, 37048–37054. [CrossRef] [PubMed]
15. Hsu, P.-C.; Wang, S.; Wu, H.; Narasimhan, V.K.; Kong, D.; Ryoung Lee, H.; Cui, Y. Performance enhancement of metal nanowire transparent conducting electrodes by mesoscale metal wires. *Nat. Commun.* **2013**, *4*, 2522. [CrossRef]
16. Wu, H.; Kong, D.; Ruan, Z.; Hsu, P.-C.; Wang, S.; Yu, Z.; Carney, T.J.; Hu, L.; Fan, S.; Cui, Y. A transparent electrode based on a metal nanotrough network. *Nat. Nanotechnol.* **2013**, *8*, 421–425. [CrossRef] [PubMed]
17. Nam, S.; Song, M.; Kim, D.-H.; Cho, B.; Lee, H.M.; Kwon, J.-D.; Park, S.-G.; Nam, K.-S.; Jeong, Y.; Kwon, S.-H.; et al. Ultrasmooth, extremely deformable and shape recoverable Ag nanowire embedded transparent electrode. *Sci. Rep.* **2014**, *4*, 4788. [CrossRef] [PubMed]
18. Kang, M.-G.; Xu, T.; Park, H.J.; Luo, X.; Guo, L.J. Efficiency enhancement of organic solar cells using transparent plasmonic Ag nanowire electrodes. *Adv. Mater.* **2010**, *22*, 4378–4383. [CrossRef]
19. Lee, P.; Lee, J.; Lee, H.; Yeo, J.; Hong, S.; Nam, K.H.; Lee, D.; Lee, S.S.; Ko, S.H. Highly stretchable and highly conductive metal electrode by very long metal nanowire percolation network. *Adv. Mater.* **2012**, *24*, 3326–3332. [CrossRef]
20. Park, M.; Kim, W.; Hwang, B.; Han, S.M. Effect of varying the density of Ag nanowire networks on their reliability during bending fatigue. *Scr. Mater.* **2019**, *161*, 70–73. [CrossRef]
21. Gao, Y.; Jiang, P.; Liu, D.F.; Yuan, H.J.; Yan, X.Q.; Zhou, Z.P.; Wang, J.X.; Song, L.; Liu, L.F.; Zhou, W.Y.; et al. Synthesis, characterization and self-assembly of silver nanowires. *Chem. Phys. Lett.* **2003**, *380*, 146–149. [CrossRef]
22. Gou, L.; Chipara, M.; Zaleski, J.M. Convenient, rapid synthesis of Ag nanowires. *Chem. Mater.* **2007**, *19*, 1755–1760. [CrossRef]
23. Jin, I.S.; Lee, H.D.; Hong, S.I.; Lee, W.; Jung, J.W. Facile post treatment of Ag nanowire/polymer composites for flexible transparent electrodes and thin film heaters. *Polymers* **2021**, *13*, 586. [CrossRef] [PubMed]
24. Chen, Z.; Boyajian, N.; Lin, Z.; Yin, R.T.; Obaid, S.N.; Tian, J.; Brennan, J.A.; Chen, S.W.; Miniovich, A.N.; Lin, L.; et al. Flexible and transparent metal nanowire microelectrode arrays and interconnects for electrophysiology, optogenetics, and optical mapping. *Adv. Mater. Technol.* **2021**, *6*, 2100225. [CrossRef]
25. Hao, T.; Wang, S.; Xu, H.; Zhang, X.; Xue, J.; Liu, S.; Song, Y.; Li, Y.; Zhao, J. Highly robust, transparent, and conductive films based on AgNW-C nanowires for flexible smart windows. *Appl. Surf. Sci.* **2021**, *559*, 149846. [CrossRef]

26. Kim, B.-J.; Shin, H.-A.S.; Jung, S.-Y.; Cho, Y.; Kraft, O.; Choi, I.-S.; Joo, Y.-C. Crack nucleation during mechanical fatigue in thin metal films on flexible substrates. *Acta Mater.* **2013**, *61*, 3473–3481. [CrossRef]
27. Lee, C.; Kim, H.; Hwang, B. Fracture behavior of metal oxide/silver nanowire composite electrodes under cyclic bending. *J. Alloy. Compd.* **2019**, *773*, 361–366. [CrossRef]
28. Oliver, W.C.; Pharr, G.M. Nanoindentation in materials research: Past, present, and future. *MRS Bull.* **2010**, *35*, 897–907. [CrossRef]
29. Schwaiger, R.; Kraft, O. Size effects in the fatigue behavior of thin Ag films. *Acta Mater.* **2003**, *51*, 195–206. [CrossRef]
30. Hwang, B.; Kim, T.; Han, S.M. Compression and tension bending fatigue behavior of Ag nanowire network. *Extrem. Mech. Lett.* **2016**, *8*, 266–272. [CrossRef]
31. Lee, J.; Lee, P.; Lee, H.; Lee, D.; Lee, S.S.; Ko, S.H. Very long Ag nanowire synthesis and its application in a highly transparent, conductive and flexible metal electrode touch panel. *Nanoscale* **2012**, *4*, 6408–6414. [CrossRef] [PubMed]
32. Nix, W.D.; Greer, J.R.; Feng, G.; Lilleodden, E.T. Deformation at the nanometer and micrometer length scales: Effects of strain gradients and dislocation starvation. *Thin Solid Film.* **2007**, *515*, 3152–3157. [CrossRef]
33. Zhu, Y.; Qin, Q.; Xu, F.; Fan, F.; Ding, Y.; Zhang, T.; Wiley, B.J.; Wang, Z.L. Size effects on elasticity, yielding, and fracture of silver nanowires: In situ experiments. *Phys. Rev. B* **2012**, *85*, 045443. [CrossRef]
34. Kim, B.-J.; Cho, Y.; Jung, M.-S.; Shin, H.-A.-S.; Moon, M.-W.; Han, H.N.; Nam, K.T.; Joo, Y.-C.; Choi, I.-S. Fatigue-free, electrically reliable copper electrode with nanohole array. *Small* **2012**, *8*, 3300–3306. [CrossRef] [PubMed]
35. Hwang, B.; Seol, J.G.; An, C.-H.; Kim, S.H. Bending fatigue behavior of silver nanowire networks with different densities. *Thin Solid Film.* **2017**, *625*, 1–5. [CrossRef]